Perceptual Grouping Reveals Distinct Roles for Sustained Slow Wave Activity and Alpha Oscillations in Working Memory

Gisella K. Diaz, Edward K. Vogel, and Edward Awh

Abstract

■ Multiple neural signals have been found to track the number of items stored in working memory (WM). These signals include oscillatory activity in the alpha band and slow-wave components in human EEG, both of which vary with storage loads and predict individual differences in WM capacity. However, recent evidence suggests that these two signals play distinct roles in spatial attention and item-based storage in WM. Here, we examine the hypothesis that sustained negative voltage deflections over parieto-occipital electrodes reflect the number of individuated items in WM, whereas oscillatory activity in the alpha frequency band (8–12 Hz) within the same electrodes tracks the attended positions in the visual display. We measured EEG activity while participants stored the orientation of visual elements that were either grouped by collinearity or not. This grouping manipulation altered the number of individuated items perceived while holding constant the number of locations occupied by visual stimuli. The negative slow wave tracked the number of items stored and was reduced in amplitude in the grouped condition. By contrast, oscillatory activity in the alpha frequency band tracked the number of positions occupied by the memoranda and was unaffected by perceptual grouping. Perceptual grouping, then, reduced the number of individuated representations stored in WM as reflected by the negative slow wave, whereas the location of each element was actively maintained as indicated by alpha power. These findings contribute to the emerging idea that distinct classes of EEG signals work in concert to successfully maintain online representations in WM. ■

INTRODUCTION

Visual working memory (VWM) is an on-line memory system that enables the rapid access and updating of information in the service of other cognitive tasks. Capacity limits in working memory (WM) exhibit robust correlations with broad measures of intellectual ability (Vogel & Awh, 2008), suggesting that WM is integral to complex cognition. Thus, there has been strong interest in delineating the behavioral and neural processes that determine these capacity limits. Multiple neural correlates have been found to monotonically scale with the number of items in visual WM up to measured storage limits (approximately 3 items), showing sustained activity over the delay period (Fukuda, Mance, & Vogel, 2015; Todd & Marois, 2004; Vogel & Machizawa, 2004). Moreover, these signals predict individual differences in visual WM capacity (Luria, Balaban, Awh, & Vogel, 2016; Fukuda et al., 2015; Vogel & Machizawa, 2004). Using scalp-EEG and the ERP technique, past work has routinely found that a contralateral and sustained negative voltage deflection, or the contralateral delay activity (CDA), shows reliable decreases in amplitude as items are added into WM (Luria et al., 2016; Vogel & Machizawa, 2004). Similarly, oscillatory activity in the alpha band has also been shown to track the number of items in WM (Sauseng et al., 2009; Busch & Herrmann, 2003). Previous work often focused on lateralized signals that required lateralized task designs and distractors to balance visual stimulation for both hemispheres. More recently, Fukuda et al. (2015) used a whole-field design that did not require distractors to examine whether whole-field signals were also sensitive to the number of items in WM. They found that parieto-occipital alpha power (7–9 Hz) and a sustained negative voltage deflection over parieto-occipital electrodes both tracked the number of items in WM.

Indeed, it has been suggested that these two signals are manifestations of the same neural process, such that amplitude modulations of oscillatory activity can explain the generation of slow evoked components, like the CDA (van Dijk, van der Werf, Mazaheri, Medendorp, & Jensen, 2010; Mazaheri & Jensen, 2008). In fact, lateralized sustained event-related fields in magnetoencephalography and lateralized alpha power were found to be strongly correlated, both spatially and temporally, in a WM task (van Dijk et al., 2010). However, the whole-field signals in Fukuda et al. (2015) showed distinct time courses and explained unique variance in predicting individual differences in WM capacity, suggesting that sustained potentials and alpha-band oscillations reflect distinct aspects of storage in visual WM (Wang, Megla,

The University of Chicago

Journal of Cognitive Neuroscience 33:7, pp. 1354–1364
https://doi.org/10.1162/jocn_a_01719

& Woodman, 2021; Hakim, Adam, Gunseli, Awh, & Vogel, 2019; Wang, Rajsic, & Woodman, 2019; Bae & Luck, 2018).

Here, we examine the hypothesis that each signal provides unique information about the contents of visual WM. Specifically, the negative slow wave can track the number of individuated items in WM, whereas parieto-occipital alpha power tracks the number of relevant locations in WM. The distinction between items and locations is a subtle distinction that has been examined before using the CDA, which was found to be sensitive to the number of items in WM regardless of the number of locations (Ikkai, McCollough, & Vogel, 2010). On the other hand, oscillatory activity in the alpha frequency band is known to track the deployment of spatial attention during storage in visual WM (Foster, Sutterer, Serences, Vogel, & Awh, 2016; Rihs, Michel, & Thut, 2007), but extant work has not discriminated between item-based and location-based explanations of this oscillatory activity. According to our hypothesis, parieto-occipital alpha power will be primarily sensitive to the number of attended locations within the visual display rather than the number of individuated items.

We used a perceptual grouping manipulation to discriminate between item-based and location-based neural activity. Past work has shown that perceptual grouping can yield strong improvements in WM performance such that a larger number of elements can be remembered when they are grouped. This effect has been observed using a variety of grouping cues, including proximity and connectedness cues (Xu, 2006; Jiang, Chun, & Olson, 2004; Woodman, Vecera, & Luck, 2003), color similarity (Morey, 2019; Gao, Gao, Tang, Shui, & Shen, 2016; Morey, Cong, Zheng, Price, & Morey, 2015; Brady & Tenenbaum, 2013; Peterson & Berryhill, 2013; Shen, Yu, Xu, & Gao, 2013; Quinlan & Cohen, 2012), shape similarity (Mate & Baqués, 2009), amodal completion (Walker & Davies, 2003), depth cues (Kristjánsson, 2006), and collinearity and closure cues (Gao et al., 2016). Here, we used collinearity cues to manipulate the number of individuated items, while holding constant the number of relevant locations. Thus, this manipulation provided traction for distinguishing between item-based and location-based neural signals.

In Experiment 1, we first establish that parieto-occipital alpha power (8–12 Hz) and the negative slow wave track the number of items stored with both color and spatial memoranda, replicating the findings of Fukuda et al. (2015) and also extending them to a spatial WM task. Our primary motivation for Experiment 1 was to ensure that both signals, especially parieto-occipital alpha power, were not disrupted by a spatial task. This anticipatory analysis was done to ensure a fair comparison between the two signals in the second experiment, where the number of items was manipulated, but the number of spatial locations was not. Specifically, we use collinearity cues to perceptually group elements in Experiment 2, while holding constant the number of elements in the display. Pairs of stimuli were either aligned to create the percept of a single item or misaligned to create the percept of two items. To anticipate the results, alpha power was sensitive to the number of locations that were attended regardless of whether the items were grouped or not, whereas the negative slow wave tracked the number of individuated items stored, revealing a smaller number of items with grouping by collinearity. These findings provide further evidence for the distinction between spatial and item-based signals in visual WM.

METHODS

Participants

Participants were recruited from the University of Chicago and the surrounding community. Overall, 16 (six women, mean age = 22 years) and 23 (14 women, mean age = 22 years) participants were run in Experiments 1 and 2, respectively. For Experiment 1, data from two participants were excluded because of the participants' voluntary withdrawal during the experiment session. In addition, data from two participants in Experiment 1 and three participants in Experiment 2 were excluded because of excessive EEG artifacts (< 150 trials remaining per condition).

Experimental procedures were approved by the institutional review board at the University of Chicago. All participants gave informed consent and were compensated for their participation at a rate of $15 per hour. Participants reported normal color vision and normal or corrected-to-normal visual acuity.

For Experiment 1, our intended sample size was 16 participants given previous research showing that this is a sufficient number of participants to observe the time course of set size effects on both the negative slow wave and parieto-occipital alpha power (Fukuda et al., 2015). However, data from four of our 16 participants were excluded from analyses given insufficient number of trials after artifact rejection or because of participants' voluntary withdrawal from the experiment session. For Experiment 2, our intended sample size was 20 participants given that our aim was to go one step further and investigate whether our set size effects were sensitive to perceptual grouping. Data from three of our initial 20 participants were excluded from our analyses after artifact rejection. We replaced these three participants and collected data from an additional three participants to complete our intended sample size.

Apparatus

Participants were tested in a dimly lit, electrically shielded chamber. Stimuli were generated using MATLAB (The Mathworks) and the Psychophysics Toolbox (Brainard, 1997; Pelli, 1997). Stimuli were presented on a 24-in.

LCD monitor (refresh rate: 120 Hz, resolution: 1080 × 1920 pixels) at a viewing distance of approximately 75 cm and against a dark gray background.

EEG Acquisition

We recorded EEG activity using 30 active Ag/AgCl electrodes mounted in an elastic cap (Brain Products actiCHamp). We recorded from International 10–20 sites Fp1, Fp2, F7, F3, Fz, F4, F8, FC5, FC1, FC2, FC6, C3, Cz, C4, CP5, CP1, CP2, CP6, P7, P3, Pz, P4, P8, PO7, PO3, PO4, PO8, O1, Oz, and O2. Two additional electrodes were placed on the left and right mastoids, and a ground electrode was placed at position Fpz. All sites were recorded with a right-mastoid reference and were rereferenced off-line to the algebraic average of the left and right mastoids. We recorded EOG using passive electrodes with a ground electrode placed on the left cheek. HEOG was recorded with a bipolar pair of electrodes placed ~1 cm from the external canthus of each eye, and vertical EOG with a bipolar pair of electrodes placed above and below the right eye. Data were filtered on-line (low cutoff = 0.01 Hz, high cutoff = 80 Hz, slope from low-to-high cutoff = 12 dB/octave) and were digitized at 500 Hz using BrainVision Recorder (Brain Products) running on a PC. During preparation, impedances were set to be below 10 kΩ.

Eyetracking

We recorded gaze position using a desk-mounted infrared eye-tracking system (EyeLink 1000 Plus, SR Research). Gaze position was sampled at 1000 Hz. Stable head position was maintained during the task using a chin rest. The eye tracker was recalibrated as needed throughout the session, including whenever participants removed their chin from the chin rest.

Artifact Rejection

For artifact rejection, each trial was segmented into −400 msec pretrial and 1750 msec poststimulus array onset epochs. We used an automated procedure to flag trials that were contaminated by ocular or EEG artifacts. Next, we used this procedure as a guideline during manual visual inspection where it was ultimately determined which trials were to be rejected. Experimenters were blind to condition when inspecting the data for artifacts. Trials contaminated by artifacts were excluded from EEG analyses but not from behavioral analyses. Participants were excluded from the final sample if they had fewer than 150 artifact-free trials per condition.

An automated artifact detection procedure was used to detect eye movements, blinks, and EEG artifacts. Trials were flagged as containing a saccade if the Euclidean vector between the mean gaze positions in the first and second halves of an 80-msec sliding window (advanced in 10-msec increments) was greater than 0.5° of visual angle. When eye tracking data were not available, we used HEOG to detect saccades. Trials were flagged as containing a saccade if the mean voltage during the first and second halves of a 150-msec sliding window (advanced in 10-msec steps) exceeded 20 μV.

For blinks, trials were flagged as containing a blink if the eye tracker could not detect the pupil at any point during the trial. When eye tracking data were not available, we used vertical EOG to detect blinks. Trials were flagged as containing a blink if the mean voltage during the first and second halves of a 150-msec sliding window (advanced in 10-msec steps) exceeded 30 μV.

For EEG artifacts, we flagged trials as containing voltage drifts (e.g., skin potentials) if the absolute change in voltage from the first quarter of the trial to the last quarter of the trial exceeded 100 μV. We flagged trials as including a sudden step in voltage (which can occur when an electrode is damaged) if the mean voltage during the first and second halves of a 250-msec sliding window (advanced in 20-msec increments) differed by more than 100 μV. We marked trials as containing high-frequency noise (e.g., muscle artifacts) if any electrode had a peak-to-peak amplitude greater than 150 μV within a 15-msec sliding window (advanced in 50-msec increments). Finally, we flagged trials as containing amplifier saturation if any electrode had 60 time points within a 200-msec sliding window (advanced in 50-msec increments) that were within 1 μV of each other.

Negative Slow Wave Analysis

EEG activity was calculated using a baseline from −400 msec to 0 msec relative to the onset of the stimulus array. The mean baseline amplitude was subtracted from EEG amplitude at each time point in the trial. The baselined trials were then averaged for each condition to create ERPs for each condition. We included 12 parieto-occipital electrodes chosen a priori and based on previous findings: P7, P3, Pz, P4, P8, PO7, PO3, PO4, PO8, O1, Oz, and O2. Statistical analyses were performed on data that were not filtered beyond the .01- to 80-Hz on-line data-acquisition filter. We low-pass filtered the data (30 Hz) for illustrative purposes in the figures.

Parieto-Occipital Alpha Power Analysis

EEG signal processing was performed in MATLAB. We band-pass filtered the raw EEG data using a filter from the FieldTrip toolbox (*ft_preproc_bandpassfilter.m*; Oostenveld, Fries, Maris, & Schoffelen, 2011) and then extracted instantaneous power values for the alpha band (8–12 Hz) by applying a Hilbert transform (*hilbert.m*) to the filtered data. We calculated alpha power for the same parieto-occipital electrodes as in the ERP analysis: P7, P3, Pz, P4, P8, PO7, PO3, PO4, PO8, O1, Oz, and O2. For illustrative purpose in the figures, we subtracted the mean

baseline (−400 to 0 msec) at each time point in the trial for each condition and converted to percent change from baseline.

Stimuli

For both experiments, a black fixation dot (diameter = 0.20°) was presented at the center of a dark gray background and remained visible for the entire trial. The stimuli were presented within a predetermined area (Experiment 1: 19.65° × 14.90°; exp. 2: 15.80° × 15.80°) and at least 0.75° (exp. 1) or 3° (exp. 2) away from fixation. During the delay interval, only the fixation dot remained on the screen. After the delay, a single probe stimulus reappeared.

For Experiment 1, the stimuli array consisted of either one or three circles (0.75°) placed randomly within a quadrant, without replacement and at least 2.25° away from each other if Set Size 3. For the color change detection task, the circles were each randomly rendered in one color from seven possible colors (red, green, blue, yellow, magenta, white, and black) without replacement. For the spatial change detection task, the circles were rendered in black. After the delay interval, a single probe stimulus reappeared that was either the "same" as one of the originally presented stimuli or "different" from any of the originally presented stimuli. For the color task, a change could occur in the color of the stimulus, whereas a change in spatial location could occur in the spatial task. Specifically, the change in spatial location could occur in any angular direction (0°–360°) and at a randomly determined distance (range: 3°–3.75°) relative to the original stimulus. The probe stimulus was constrained to its original quadrant and had to maintain the same minimum distance requirement (2.25°) from the original stimuli locations.

For Experiment 2, the stimuli array consisted of either two or four black circles (3°) with rectangular gaps. The locations of the stimuli were assigned in a serial manner. The location of the first stimulus was randomly selected to fall within the predetermined bounds. In relation to the first stimulus, the location of the second stimulus could occur in a randomly determined angular direction (0°–360°) and 5.65° away from the first stimulus, while maintaining the requirements of the first stimulus (i.e., remaining within the predetermined bounds), and effectively forming a pair. For Set Size 4, the third and fourth stimuli locations were determined in a similar manner with the additional constraints that stimuli be at least 6° away from stimuli belonging to a different pair and that pairs of stimuli did not intersect. On half of the trials, the gaps of each pair of stimuli were oriented toward each other to form the percept of either one (Set Size 2) or two (Set Size 4) items (grouped condition). On the remaining trials, the gaps were misaligned (ungrouped condition). The same location configurations were used across conditions (grouped and ungrouped) but were unique for each participant. To avoid accidental pairs in the ungrouped condition, the orientation of the second stimulus in each pair had to be more than 5° clockwise or counterclockwise from the orientation it would be in the grouped condition.

Experiment 1 Procedure

Participants performed a whole-field change detection task (Figure 1A and 1B). The trial began with a fixation dot presented at the center of the screen for a randomly

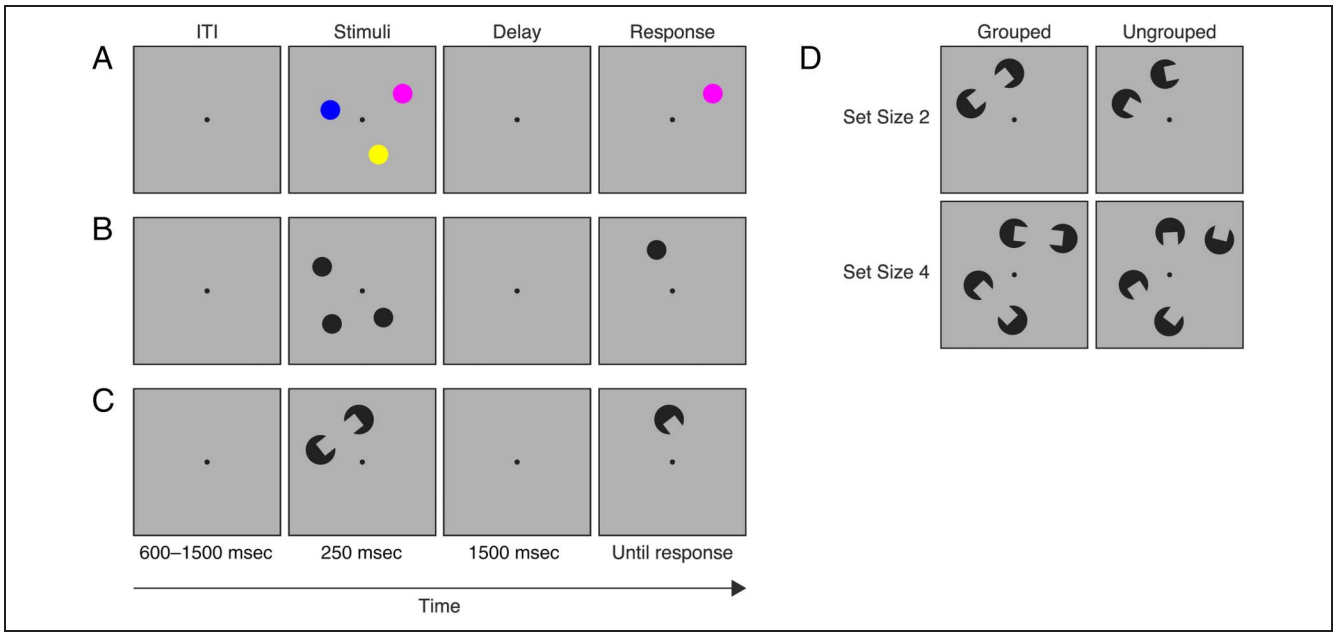

Figure 1. Color (A) and spatial (B) change detection tasks from Experiment 1. Perceptual grouping change detection task from Experiment 2 (C) with example stimuli displays for each of the four conditions (D). ITI = intertrial interval.

determined duration between 600 and 1500 msec. A stimuli array followed and was presented for 250 msec. The stimuli array consisted of either one or three circles that were either rendered in color (color change detection task) or in black (spatial change detection task). Participants were asked to remember as many of the stimuli as possible over a 1500-msec blank delay interval. After the delay, a single stimulus reappeared. Participants used a keyboard button press to indicate whether this probe stimulus was presented at one of the previously occupied locations. For the color task (Figure 1A), a change could occur in the color of the stimulus, whereas a change in spatial location could occur in the spatial task (Figure 1B). Participants pressed the "z" or "/" key to indicate whether the probe stimulus was the "same" or "different," respectively, from the stimuli display. There were no practice trials given before the formal experiment. Participants were given verbal and written task instructions with the aid of an example trial image similar to Figure 1A–C.

Within a block, half of the trials were "same" trials, and the remaining half were "different" trials. Similarly, half of the trials were Set Size 1, and the remaining half were Set Size 3. Participants completed 20 blocks with each containing 60 trials of either the color or spatial change detection task. There were an equal number of color and spatial change detection blocks, which were completed in an alternating order. The task for the first block was counterbalanced across participants. Participants self-initiated each block by pressing the spacebar key. The experiment session was scheduled to take 3 hr, but the actual duration of the session (~2.5–3.5 hr) depended on each participant's pace because they initiated each block and decided when (and if) to take breaks between blocks.

Experiment 2 Procedure

The procedure was similar to Experiment 1 with the following exceptions. The stimuli array consisted of either two or four black circles with rectangular gaps (Figure 1C). On half of the trials, the gaps of each pair of stimuli were oriented toward each other to form the percept of either one (Set Size 2) or two (Set Size 4) items. On the remaining trials, the gaps were misaligned (Figure 1D). After the delay, participants indicated whether the orientation of the probe stimulus that reappeared was the "same" or "different." Half of the trials were Set Size 2, and the remaining half were Set Size 4. Participants completed 30 blocks of 40 trials each. The experiment session was scheduled to take 3.5 hr (~3–4 hr).

Experimental Design and Statistical Analysis

Both experiments used a 2 × 2 within-subject design. For Experiment 1, the factors were set size (1 or 3) and task type (color or spatial). The type of task alternated with each block. For Experiment 2, the factors were set size (2 or 4) and grouping condition (grouped or ungrouped).

Behavioral data were analyzed using a repeated-measures ANOVA. Neural data were analyzed using repeated-measures ANOVAs on averaged delay activity data and cluster-based permutation tests (Sassenhagen & Draschkow, 2019; Maris & Oostenveld, 2007) on data averaged over parieto-occipital electrodes. In Experiment 1, our focus was on ANOVAs given that we were investigating robust set size effects that had been observed before. In Experiment 2, we focused on cluster-based permutation tests to search for novel grouping effects in a data-driven way. For consistency, we present results using both approaches for each experiment. For the cluster-based permutation tests, we first reduced our high-dimensional data (n time points × n participants; per condition) to a single value. Repeated-measures t tests were calculated at each time point to assess the difference between conditions (e.g., Set Size 1 vs. Set Size 3), which resulted in a map of t scores across time. Time points were thresholded according to an a priori defined criterion (which corresponded to a p value of .05, two-sided), and adjacent time points with t scores that exceeded this value were grouped together to form a cluster. Clusters were summarized into a single number by summing the t values, which produced a single value for each cluster. It is important to note that the extent of the cluster became fixed at the end of this first step and individual time points were not visible to the next inference step. Specifically, the cluster structure was our only test statistic and no statistical inference was made about individual time points. Nevertheless, we next calculated the probability that these values came from a null distribution. Permutation tests were used to establish the probability of our data under the null hypothesis given that it is unclear what distribution of t value sums would be expected under the null hypothesis. The number of permutations was 10,000 or the maximum possible, whichever was lowest. On each iteration and for each time point, it was randomly determined if the first condition was subtracted from the second condition or vice versa for each participant. Then for each iteration, the cluster formation step was repeated. The cluster with the highest sum of t values was identified, and the sum of its t values was stored and became our surrogate-null value for that permutation. After all iterations, the cumulative density of these surrogate-null values was our approximation of the values under the null hypothesis. The p value then was calculated as the percentage of surrogate-null values that the observed data exceeded.

RESULTS

Experiment 1

There was a main effect of Set Size, $F(1, 11) = 17.99$, $p = .001$, $\eta^2 = .62$, and Task, $F(1, 11) = 8.18$, $p = .016$, $\eta^2 = .43$, on accuracy, such that accuracy was higher for Set Size 1 ($M = 0.95$, $SD = 0.05$) than Set Size 3 ($M = 0.90$,

SD = 0.08) and for the color task (M = 0.94, SD = 0.05) than the spatial task (M = 0.90, SD = 0.08). There was no significant interaction between Set Size and Task on accuracy, $F(1, 11) = 0.05$, $p = .84$, $\eta^2 = .004$.

We used repeated-measures ANOVAs on averaged delay activity from parieto-occipital electrodes to analyze the effects of Set Size and Task Type on both the negative slow wave and parieto-occipital alpha power. Moreover, we used nonparametric cluster-based permutation tests (Maris & Oostenveld, 2007) to corroborate the effects of Set Size and Task Type in a more nuanced manner. Given previous research (Fukuda et al., 2015), we predicted that both signals would show characteristic set size effects. Specifically, Fukuda et al. (2015) found a monotonic increase in slow wave negativity and a monotonic decrease in parieto-occipital alpha power with increases in set size up to typical capacity (approximately 3 items).

The negative slow wave and parieto-occipital alpha power were analyzed during the delay period (250–1750 msec). As predicted, there was a main effect of Set Size on voltage at parieto-occipital electrodes (Figure 2A; $F(1, 11) = 16.99$, $p = .002$, $\eta^2 = .61$), such that the amplitude was more negative for Set Size 3 than Set Size 1. There was no main effect of Task, $F(1, 11) = 0.47$, $p = .51$, $\eta^2 = .04$, and no significant interaction, $F(1, 11) = 0.29$, $p = .60$, $\eta^2 = .03$. Cluster-based permutation tests echoed these findings. Three clusters in the voltage at parieto-occipital electrodes were found to be sensitive to set size and extended from ~130 to ~210 msec, ~490 to ~1020 msec, ~1020 to ~1190 msec. The permutation test indicated that the effects of Set Size were significant ($p = .048$, $p = .007$, $p = .044$). There were no clusters that were sensitive to Task Type. In short, we replicated and extended previous findings that the negative slow wave is sensitive to set size in a color change detection task (Fukuda et al., 2015), as well as in a spatial change detection task.

The main effect of Set Size on parieto-occipital alpha power did not reach significance when averaging over the entire delay interval (Figure 2B; $F(1, 11) = 3.06$, $p = .11$, $\eta^2 = .22$), although an early transient effect of Set Size was evident with more alpha power suppression for Set Size 3 than Set Size 1. There was a main effect of Task, $F(1, 11) = 6.83$, $p = .024$, $\eta^2 = .38$, which was driven by the rapid return to baseline in the color task for Set Size 3 trials. Importantly, the interaction did not reach significance, $F(1, 11) = 1.03$, $p = .33$, $\eta^2 = .09$. Cluster-based permutation tests revealed more nuanced results. There was a cluster sensitive to set size that extended from ~−30 to ~870 msec. The permutation test indicated that there was a significant effect of Set Size ($p = .006$). There was also a cluster that was sensitive to task, extending from ~680 to ~1560 msec. The permutation test indicated a significant effect of task ($p = .003$). Thus, we again replicated

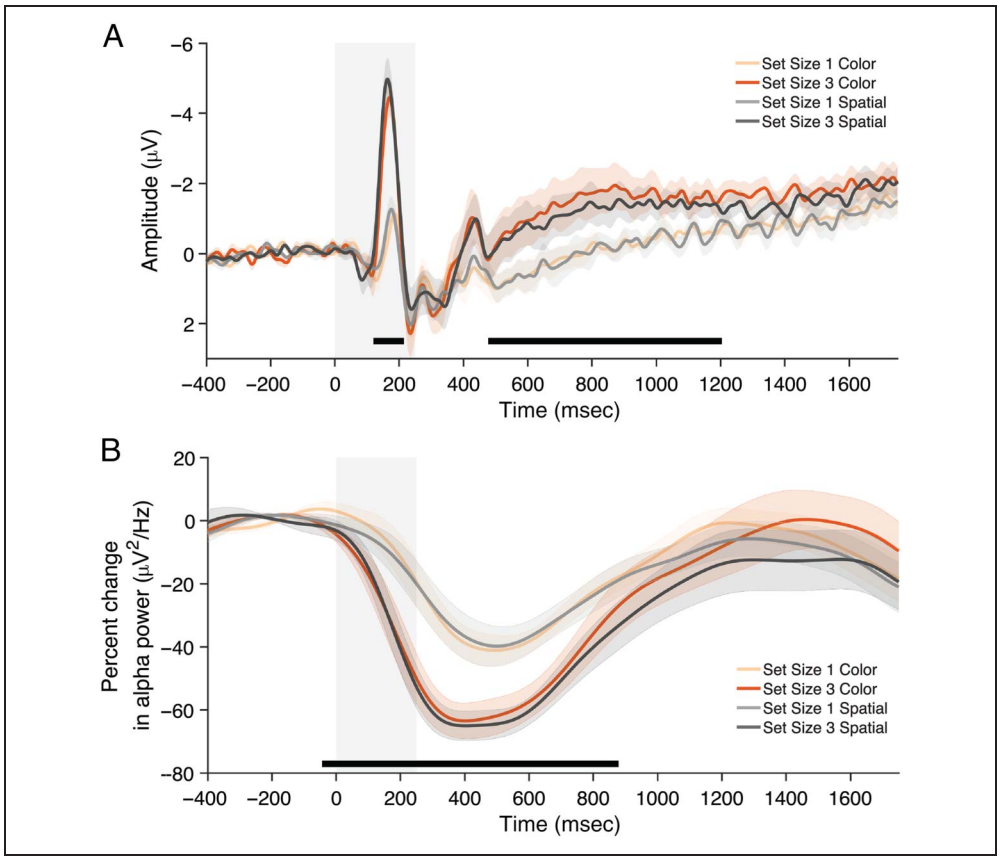

Figure 2. Averaged negative slow wave (A) and averaged alpha power suppression (B) observed at parieto-occipital electrodes in Experiment 1. Shaded regions indicate duration of stimuli display. Black bars indicate clusters showing a significant ($p < .05$) Set Size effect from cluster-based permutations tests.

previous findings from Fukuda et al. (2015) that parieto-occipital alpha power shows a monotonic decrease with an increase in set size for both a color and spatial change detection task.

In summary, our findings from Experiment 1 replicate those of Fukuda et al. (2015) and extend them to spatial memoranda. For both color and spatial memoranda, both the negative slow wave and parieto-occipital alpha power are sensitive to set size. In Experiment 2, we investigate whether these set size effects are further shaped by collinearity cues. Do grouping cues that compel the perception of fewer individuated objects also affect the magnitude of these storage-related signals?

Experiment 2

There was a main effect of Set Size, $F(1, 19) = 110.3$, $p < .001$, $\eta^2 = .85$, and Grouping, $F(1,19) = 146.7$, $p < .001$, $\eta^2 = .89$, on accuracy, such that accuracy was higher for Set Size 2 ($M = 0.94$, $SD = 0.05$) than Set Size 4 ($M = 0.86$, $SD = 0.10$) and for grouped trials ($M = 0.95$, $SD = 0.05$) compared to ungrouped trials ($M = 0.85$, $SD = 0.10$). There was also a significant interaction between Set Size and Grouping on accuracy, $F(1,19) = 116.1$, $p < .001$, $\eta^2 = .86$, such that there was a greater benefit of grouping for Set Size 4 than Set Size 2.

Nonparametric cluster-based permutation tests were used to analyze the effects of set size and grouping on both the negative slow wave and parieto-occipital alpha power. In comparison to Experiment 1, the grouping effects of interest in Experiment 2 were more novel and the timing and duration of any grouping effect was not known. Accordingly, choosing an objective window of interest for ANOVAs was not possible. Instead, we focused on cluster-based permutation tests; however, we also report the results of repeated-measures ANOVAs using averaged delay activity from three equally sized windows of 500 msec each (early, middle, and late delay).

Given previous research and our own data, we again predicted that both signals would show characteristic set size effects, with higher slow wave negativity and reduced alpha power for Set Size 4 compared to Set Size 2. The central question of the study, however, was to investigate whether these signals were sensitive to grouping when set size effects were present. To this end, we first identified clusters that were sensitive to set size and then examined whether those clusters were also sensitive to grouping.

First, there was a main effect of Set Size and Grouping on voltage at parieto-occipital electrodes during the early time window (250–750 msec; Table 1). A cluster in the voltage at parieto-occipital electrodes extended from ~330 to ~880 msec. The cluster-based permutation test indicated that there was a significant effect of Set Size (Figure 3A; $p = .005$), such that amplitude was more negative for Set Size 4 than Set Size 2. Within this cluster, another cluster was identified that extended from ~370

Table 1. Repeated-Measures ANOVAs for Neural Data in Experiment 2

Terms	*F-statistics*	*df1*	*df2*	*p Value*	η^2
Negative Slow Wave					
Early (250–750 msec)					
Set Size (2, 4)	22.21	1	19	<.001	.54
Condition (Ingrouped to Ungrouped)	9.11	1	19	.007	.32
Set Size × Condition	3.07	1	19	.10	.14
Middle (750–1250 msec)					
Set Size (2, 4)	5.11	1	19	.036	.21
Condition (Grouped, Ungrouped)	3.49	1	19	.077	.16
Set Size × Condition	2.39	1	19	.14	.11
Late (1250–1750 msec)					
Set Size (2, 4)	3.33	1	19	.084	.15
Condition (Grouped, Ungrouped)	0.64	1	19	.43	.03
Set Size × Condition	2.76	1	19	.11	.13
Alpha Power					
Early (250–750 msec)					
Set Size (2, 4)	14.51	1	19	.001	.43
Condition (Grouped, Ungrouped)	2.97	1	19	.10	.14
Set Size × Condition	0.08	1	19	.78	.00
Middle (750–1250 msec)					
Set Size (2, 4)	10.32	1	19	.005	.35
Condition (Grouped, Ungrouped)	3.01	1	19	.10	.14
Set Size × Condition	4.89	1	19	.04	.21
Late (1250–1750 msec)					
Set Size (2, 4)	2.61	1	19	.12	.12
Condition (Grouped, Ungrouped)	0.58	1	19	.46	.03
Set Size × Condition	3.84	1	19	.065	.17

We applied 2 (Set Size 2, 4) × 2 (Grouped, Ungrouped) repeated-measures ANOVAs to voltage and alpha power at parieto-occipital electrodes averaging over delay activity in three equally sized windows of 500 msec each. Significant ($p < .0167$; Bonferroni-corrected for $\alpha = .05$) effects in **bold**.

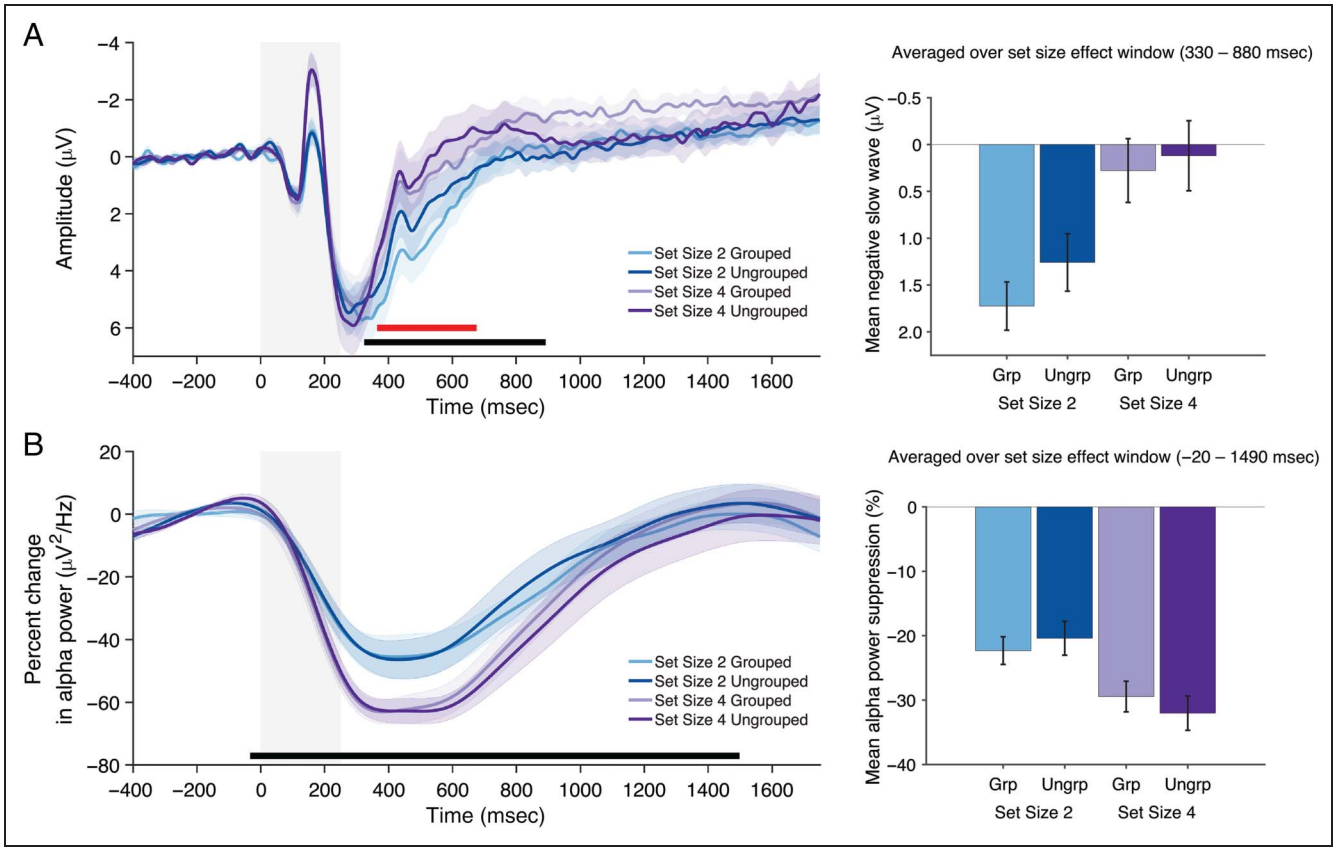

Figure 3. Averaged negative slow wave (A) and averaged alpha power suppression (B) observed at parieto-occipital electrodes in Experiment 2. Shaded regions indicate duration of stimuli display. Black and red bars indicate clusters showing a significant ($p < .05$) set size or grouping effect, respectively, from cluster-based permutation tests.

to ~670 msec. The permutation test indicated that there was a significant effect of Grouping ($p < .001$), such that amplitude was more negative when stimuli were ungrouped relative to grouped. To assess the evidence for grouping during this set size window, estimated Bayes factors were calculated ($BF_{01} = 0.89$) and indicated that the data were 1.13 times more likely to have occurred under the alternative hypothesis.

Thus, we first replicated our finding from Experiment 1 that the negative slow wave was modulated by set size. Moreover, we extended those findings by demonstrating that the negative slow wave was also modulated by grouping. The reduction in amplitude of the negative slow wave for grouped stimuli is consistent with our hypothesis that the negative slow wave tracks the number of individuated items.

Halfway through the delay, we observed an unexpected drop in amplitude in the negative slow wave for Set Size 4 Ungrouped, such that the set size effect was eliminated. Although the mechanisms involved are unknown, it is possible that this pattern is because of the strategic reorienting of attention to the remembered items within capacity. In line with this speculation, we found that the drop in the negative slow wave was restricted to participants with high Set Size 4 Ungrouped performance, which is consistent with the idea of strategic refocusing. Additional work is needed to bolster the findings of this post hoc analysis.

In alpha power, there was a main effect of Set Size during the early and middle time windows (250–750 msec, 750–1250 msec; Table 1), but no main effect of Grouping. A cluster extended from ~−20 to ~1490 msec with the permutation test indicating that there was a significant effect of Set Size (Figure 3B; $p < .001$), such that alpha power was lower for Set Size 4 than Set Size 2. Despite this robust effect of the number of positions, however, no clusters showing this set size effect were sensitive to the effects of perceptual grouping. Estimated Bayes factors during this set size window were calculated ($BF_{01} = 1.51$) and indicated that the data were 1.5 times more likely to have occurred under the null hypothesis. This suggests that participants maintained their attention on the same number of positions, even though the number of individuated items stored was reduced in the grouped condition.

DISCUSSION

In line with previous research, perceptual grouping cues enhanced VWM performance and also led to distinct changes in EEG signals that track WM storage.

Specifically, the negative slow wave—a signal known to track the number of items stored in visual WM (Fukuda et al., 2015)—was reduced in amplitude for grouped stimuli, consistent with the idea that grouping reduces the number of individuated items. By contrast, parieto-occipital alpha power reliably tracked the number of locations that were attended, but this signal was completely unaffected by perceptual grouping. This pattern of results suggests that the negative slow wave is sensitive to the number of individuated items in WM, whereas parieto-occipital alpha power tracks the number of visually attended locations.

These diverging effects of perceptual grouping dovetail with recent evidence showing that the EEG signals that track WM storage fall into at least two distinct classes. Although both parieto-occipital slow waves and alpha power track the number of relevant items in a WM task, they have distinct temporal profiles, and explain distinct between-subjects variance in WM capacity (Fukuda et al., 2015). Moreover, these two EEG signals respond distinctly to manipulations of attentional priority in WM (Günseli et al., 2019) and to whether the task motivates the maintenance of item-based information (Hakim et al., 2019).

The perceptual grouping effect on the negative slow wave is similar to the effects reported in studies that examined CDA, a lateralized ERP component that is observed at similar electrode sites as the negative slow wave and is highly sensitive to the number of items in VWM (Luria et al., 2016; Vogel & Machizawa, 2004). Previous research characterizing the negative slow wave was driven by the goal of finding a whole-field alternative to the CDA that would not require the filtering of distractors (Fukuda et al., 2015). The findings, so far, are consistent with the hypothesis that the CDA and negative slow wave are indexing the same neural operation, although further work is needed to determine how these signals are related. That said, previous research shows that the CDA tracks the number of items regardless of the number of relevant locations and even as the items undergo physical transformations. For instance, the CDA reliably tracks additional items that are added into VWM regardless of whether these additional items are presented in the same locations as previously encoded memoranda or not, which suggests that it ultimately tracks the number of items rather than the number of attended positions (Ikkai et al., 2010). Moreover, the CDA is sensitive to common fate cues, such that there is a reduction in the CDA when common motion cues encourage the perception of multiple elements as a single item (Luria & Vogel, 2014). There is also a reduction in the CDA for identical colors relative to distinct colors, which suggests that identical colors might be maintained as a group in VWM (Peterson, Gözenman, Arciniega, & Berryhill, 2015; Gao et al., 2011).

Importantly, the current work extends these findings by providing a direct measure of information maintained about each of the grouped elements, specifically spatial information. Alpha oscillations provided a sensitive index of the number of attended positions and revealed that perceptual grouping yielded no reduction in the number of attended positions. Specifically, parieto-occipital alpha power continued to index the same number of spatial locations even when the stimuli were grouped, which suggests that both constituents of the group were maintained. This finding rules out the possibility that participants maintained only half of the group in grouped trials and used that information to inform their decision at the time of response. Instead, perceptual grouping boosted orientation WM performance by reducing the number of individuated representations stored without sacrificing spatial information about each of the grouped elements. Our findings are broadly consistent with past work that found a reduced CDA for identical colors presumably maintained as a group (Peterson et al., 2015; Gao et al., 2011). Future research could extend the current work to include these similarity cues or other grouping cues that are especially compelling, such as common onset or common fate, or cues that have been found to boost WM performance, such as proximity (e.g., Woodman et al., 2003).

Finally, the distinct effects of perceptual grouping on item-based and spatial EEG signals are consistent with a broad class of models that distinguish between the number of individuated objects maintained in WM and the specific featural information that is stored about each of those objects (Fukuda, Vogel, Mayr, & Awh, 2010; Awh, Barton, & Vogel, 2007; Xu & Chun, 2006). For example, Xu and Chun (2009) described a neural object file theory that distinguishes between an initial stage of object individuation and a subsequent stage in which the details of the individuated objects are apprehended. This account is supported by their finding that grouped objects elicited lower fMRI responses in inferior intraparietal sulcus (a brain region thought to track the number of individuated items in WM) but higher responses in superior intraparietal sulcus and the lateral occipital complex, regions that are thought to be sensitive to the information load or complexity of the stored items (Xu & Chun, 2007). According to the neural object file account, grouping reduced the number of individuated items in a capacity-limited individuation stage, allowing more information to be relayed to higher visual areas in the identification stage. Our results bolster this interpretation by showing that distinct neural signals track the number of individuated items in WM and the details of the specific locations associated with each item. Thus, although neural signals tracking WM storage are sometimes viewed in a monolithic fashion, there is growing evidence that distinct delay signals with distinct computational roles work in parallel to maintain information in an on-line state (Hakim, Awh, & Vogel, 2021).

Acknowledgments

Research was supported by National Institute of Mental Health grant ROI MH087214 and Office of Naval Research grant N00014-12-1-0972. We thank Ariana Gale and Clara Sava-Segal for assistance with data collection.

Reprint requests should be sent to Gisella K. Diaz, Department of Psychology, The University of Chicago, 940 East 57th Street, Chicago, IL 60637, or via e-mail: gisella@uchicago.edu.

Funding Information

Edward K. Vogel, Office of Naval Research (https://dx.doi.org/10.13039/100000006), grant number: N00014-12-1-0972. Gisella K. Diaz and Edward K. Vogel, National Institute of Mental Health (https://dx.doi.org/10.13039/100000025), grant number: ROI MH087214.

Diversity in Citation Practices

A retrospective analysis of the citations in every article published in this journal from 2010 to 2020 has revealed a persistent pattern of gender imbalance: Although the proportions of authorship teams (categorized by estimated gender identification of first author/last author) publishing in the *Journal of Cognitive Neuroscience (JoCN)* during this period were M(an)/M = .408, W(oman)/M = .335, M/W = .108, and W/W = .149, the comparable proportions for the articles that these authorship teams cited were M/M = .579, W/M = .243, M/W = .102, and W/W = .076 (Fulvio et al., *JoCN*, 33:1, pp. 3–7). Consequently, *JoCN* encourages all authors to consider gender balance explicitly when selecting which articles to cite and gives them the opportunity to report their article's gender citation balance.

REFERENCES

Awh, E., Barton, B., & Vogel, E. K. (2007). Visual working memory represents a fixed number of items regardless of complexity. *Psychological Science*, *18*, 622–628. https://doi.org/10.1111/j.1467-9280.2007.01949.x, PubMed: 17614871

Bae, G.-Y., & Luck, S. J. (2018). Dissociable decoding of spatial attention and working memory from EEG oscillations and sustained potentials. *Journal of Neuroscience*, *38*, 409–422. https://doi.org/10.1523/JNEUROSCI.2860-17.2017, PubMed: 29167407

Brady, T. F., & Tenenbaum, J. B. (2013). A probabilistic model of visual working memory: Incorporating higher order regularities into working memory capacity estimates. *Psychological Review*, *120*, 85–109. https://doi.org/10.1037/a0030779, PubMed: 23230888

Brainard, D. H. (1997). The Psychophysics Toolbox. *Spatial Vision*, *10*, 433–436. https://doi.org/10.1163/156856897X00357, PubMed: 9176952

Busch, N. A., & Herrmann, C. S. (2003). Object-load and feature-load modulate EEG in a short-term memory task. *NeuroReport*, *14*, 1721–1724. https://doi.org/10.1097/00001756-200309150-00013, PubMed: 14512845

Foster, J. J., Sutterer, D. W., Serences, J. T., Vogel, E. K., & Awh, E. (2016). The topography of alpha-band activity tracks the content of spatial working memory. *Journal of Neurophysiology*, *115*, 168–177. https://doi.org/10.1152/jn.00860.2015, PubMed: 26467522

Fukuda, K., Mance, I., & Vogel, E. K. (2015). α power modulation and event-related slow wave provide dissociable correlates of visual working memory. *Journal of Neuroscience*, *35*, 14009–14016. https://doi.org/10.1523/JNEUROSCI.5003-14.2015, PubMed: 26468201

Fukuda, K., Vogel, E., Mayr, U., & Awh, E. (2010). Quantity, not quality: The relationship between fluid intelligence and working memory capacity. *Psychonomic Bulletin & Review*, *17*, 673–679. https://doi.org/10.3758/17.5.673, PubMed: 21037165

Gao, Z., Gao, Q., Tang, N., Shui, R., & Shen, M. (2016). Organization principles in visual working memory: Evidence from sequential stimulus display. *Cognition*, *146*, 277–288. https://doi.org/10.1016/j.cognition.2015.10.005, PubMed: 26500190

Gao, Z., Xu, X., Chen, Z., Yin, J., Shen, M., & Shui, R. (2011). Contralateral delay activity tracks object identity information in visual short term memory. *Brain Research*, *1406*, 30–42. https://doi.org/10.1016/j.brainres.2011.06.049, PubMed: 21757188

Günseli, E., Fahrenfort, J. J., van Moorselaar, D., Daoultzis, K. C., Meeter, M., & Olivers, C. N. L. (2019). EEG dynamics reveal a dissociation between storage and selective attention within working memory. *Scientific Reports*, *9*, 13499. https://doi.org/10.1038/s41598-019-49577-0, PubMed: 31534150

Hakim, N., Adam, K. C. S., Gunseli, E., Awh, E., & Vogel, E. K. (2019). Dissecting the neural focus of attention reveals distinct processes for spatial attention and object-based storage in visual working memory. *Psychological Science*, *30*, 526–540. https://doi.org/10.1177/0956797619830384, PubMed: 30817220

Hakim, N., Awh, E., & Vogel, E. K. (2021). Manifold visual working memory. In R. H. Logie, V. Camos, & N. Cowan (Eds.), *Working memory: State of the science* (pp. 44–84). Oxford: Oxford University Press. https://doi.org/10.1093/oso/9780198842286.003.0011

Ikkai, A., McCollough, A. W., & Vogel, E. K. (2010). Contralateral delay activity provides a neural measure of the number of representations in visual working memory. *Journal of Neurophysiology*, *103*, 1963–1968. https://doi.org/10.1152/jn.00978.2009, PubMed: 20147415

Jiang, Y., Chun, M. M., & Olson, I. R. (2004). Perceptual grouping in change detection. *Perception & Psychophysics*, *66*, 446–453. https://doi.org/10.3758/BF03194892, PubMed: 15283069

Kristjánsson, Á. (2006). Surface assignment modulates object formation for visual short-term memory. *Perception*, *35*, 865–881. https://doi.org/10.1068/p5526, PubMed: 16970197

Luria, R., Balaban, H., Awh, E., & Vogel, E. K. (2016). The contralateral delay activity as a neural measure of visual working memory. *Neuroscience and Biobehavioral Reviews*, *62*, 100–108. https://doi.org/10.1016/j.neubiorev.2016.01.003, PubMed: 26802451

Luria, R., & Vogel, E. K. (2014). Come together, right now: Dynamic overwriting of an object's history through common fate. *Journal of Cognitive Neuroscience*, *26*, 1819–1828. https://doi.org/10.1162/jocn_a_00584, PubMed: 24564468

Maris, E., & Oostenveld, R. (2007). Nonparametric statistical testing of EEG- and MEG-data. *Journal of Neuroscience Methods*, *164*, 177–190. https://doi.org/10.1016/j.jneumeth.2007.03.024, PubMed: 17517438

Mate, J., & Baqués, J. (2009). Visual similarity at encoding and retrieval in an item recognition task. *Quarterly Journal of Experimental Psychology*, *62*, 1277–1284. https://doi.org/10.1080/17470210802680769, PubMed: 19235099

Mazaheri, A., & Jensen, O. (2008). Asymmetric amplitude modulations of brain oscillations generate slow evoked responses. *Journal of Neuroscience*, *28*, 7781–7787. https://doi.org/10.1523/JNEUROSCI.1631-08.2008, PubMed: 18667610

Morey, C. C. (2019). Perceptual grouping boosts visual working memory capacity and reduces effort during retention. *British*

Journal of Psychology, *110*, 306–327. https://doi.org/10.1111/bjop.12355, PubMed: 30345501
Morey, C. C., Cong, Y., Zheng, Y., Price, M., & Morey, R. D. (2015). The color-sharing bonus: Roles of perceptual organization and attentive processes in visual working memory. *Archives of Scientific Psychology*, *3*, 18–29. https://doi.org/10.1037/arc0000014
Oostenveld, R., Fries, P., Maris, E., & Schoffelen, J.-M. (2011). FieldTrip: Open source software for advanced analysis of MEG, EEG, and invasive electrophysiological data. *Computational Intelligence and Neuroscience*, *2011*, 156869. https://doi.org/10.1155/2011/156869, PubMed: 21253357
Pelli, D. G. (1997). The VideoToolbox software for visual psychophysics: Transforming numbers into movies. *Spatial Vision*, *10*, 437–442. https://doi.org/10.1163/156856897X00366, PubMed: 9176953
Peterson, D. J., & Berryhill, M. E. (2013). The Gestalt principle of similarity benefits visual working memory. *Psychonomic Bulletin & Review*, *20*, 1282–1289. https://doi.org/10.3758/s13423-013-0460-x, PubMed: 23702981
Peterson, D. J., Gözenman, F., Arciniega, H., & Berryhill, M. E. (2015). Contralateral delay activity tracks the influence of Gestalt grouping principles on active visual working memory representations. *Attention, Perception, & Psychophysics*, *77*, 2270–2283. https://doi.org/10.3758/s13414-015-0929-y, PubMed: 26018644
Quinlan, P. T., & Cohen, D. J. (2012). Grouping and binding in visual short-term memory. *Journal of Experimental Psychology: Learning, Memory, and Cognition*, *38*, 1432–1438. https://doi.org/10.1037/a0027866, PubMed: 22449133
Rihs, T. A., Michel, C. M., & Thut, G. (2007). Mechanisms of selective inhibition in visual spatial attention are indexed by alpha-band EEG synchronization. *European Journal of Neuroscience*, *25*, 603–610. https://doi.org/10.1111/j.1460-9568.2007.05278.x, PubMed: 17284203
Sassenhagen, J., & Draschkow, D. (2019). Cluster-based permutation tests of MEG/EEG data do not establish significance of effect latency or location. *Psychophysiology*, *56*, e13335. https://doi.org/10.1111/psyp.13335, PubMed: 30657176
Sauseng, P., Klimesch, W., Heise, K. F., Gruber, W. R., Holz, E., Karim, A. A., et al. (2009). Brain oscillatory substrates of visual short-term memory capacity. *Current Biology*, *19*, 1846–1852. https://doi.org/10.1016/j.cub.2009.08.062, PubMed: 19913428
Shen, M., Yu, W., Xu, X., & Gao, Z. (2013). Building blocks of visual working memory: Objects or Boolean maps? *Journal of Cognitive Neuroscience*, *25*, 743–753. https://doi.org/10.1162/jocn_a_00348, PubMed: 23249354
Todd, J. J., & Marois, R. (2004). Capacity limit of visual short-term memory in human posterior parietal cortex. *Nature*, *428*, 751–754. https://doi.org/10.1038/nature02466, PubMed: 15085133
van Dijk, H., van der Werf, J., Mazaheri, A., Medendorp, W. P., & Jensen, O. (2010). Modulations in oscillatory activity with amplitude asymmetry can produce cognitively relevant event-related responses. *Proceedings of the National Academy of Sciences, U.S.A.*, *107*, 900–905. https://doi.org/10.1073/pnas.0908821107, PubMed: 20080773
Vogel, E. K., & Awh, E. (2008). How to exploit diversity for scientific gain: Using individual differences to constrain cognitive theory. *Current Directions in Psychological Science*, *17*, 171–176. https://doi.org/10.1111/j.1467-8721.2008.00569.x
Vogel, E. K., & Machizawa, M. G. (2004). Neural activity predicts individual differences in visual working memory capacity. *Nature*, *428*, 748–751. https://doi.org/10.1038/nature02447, PubMed: 15085132
Walker, P., & Davies, S. J. (2003). Perceptual completion and object-based representations in short-term visual memory. *Memory & Cognition*, *31*, 746–760. https://doi.org/10.3758/BF03196113, PubMed: 12956239
Wang, S., Megla, E. E., & Woodman, G. F. (2021). Stimulus-induced alpha suppression tracks the difficulty of attentional selection, not visual working memory storage. *Journal of Cognitive Neuroscience*, *33*, 536–562. https://doi.org/10.1162/jocn_a_01637, PubMed: 33054550
Wang, S., Rajsic, J., & Woodman, G. F. (2019). The contralateral delay activity tracks the sequential loading of objects into visual working memory, unlike lateralized alpha oscillations. *Journal of Cognitive Neuroscience*, *31*, 1689–1698. https://doi.org/10.1162/jocn_a_01446, PubMed: 31274391
Woodman, G. F., Vecera, S. P., & Luck, S. J. (2003). Perceptual organization influences visual working memory. *Psychonomic Bulletin & Review*, *10*, 80–87. https://doi.org/10.3758/BF03196470, PubMed: 12747493
Xu, Y. (2006). Understanding the object benefit in visual short-term memory: The roles of feature proximity and connectedness. *Perception & Psychophysics*, *68*, 815–828. https://doi.org/10.3758/BF03193704, PubMed: 17076349
Xu, Y., & Chun, M. M. (2006). Dissociable neural mechanisms supporting visual short-term memory for objects. *Nature*, *440*, 91–95. https://doi.org/10.1038/nature04262, PubMed: 16382240
Xu, Y., & Chun, M. M. (2007). Visual grouping in human parietal cortex. *Proceedings of the National Academy of Sciences, U.S.A.*, *104*, 18766–18771. https://doi.org/10.1073/pnas.0705618104, PubMed: 17998539
Xu, Y., & Chun, M. M. (2009). Selecting and perceiving multiple visual objects. *Trends in Cognitive Sciences*, *13*, 167–174. https://doi.org/10.1016/j.tics.2009.01.008, PubMed: 19269882